ELSEVIER

Electric Power Systems Research 54 (2000) 131–138

ELECTRIC POWER SYSTEMS RESEARCH

www.elsevier.com/locate/epsr

Impedances for the calculation of electromagnetic transient phenomena and resonance in transformer windings

Enrique Mombello [a,*], Klaus Möller [b]

[a] *Institudo de Engeriá Eléctrica, Universidad Nacional de San Juan Consejo de Investigaciones Científicas y Técnicas (CONICET), Av. Lib. Gra. San Martin 1190 oeste 5400 San Juan, Argentina*

[b] *Institut für Allgemeine Elektrotechnik und Hochspannungstechnik, Rhein.-West. Techn. Hochschule, Schinkelstrasse 2, 52056, Aachen, Germany*

Received 3 March 1999; received in revised form 25 June 1999; accepted 15 September 1999

Abstract

In this paper the authors look for a better understanding of the properties of the impedances of transformer windings. These impedances are very important for the calculation of the resonant behavior of transformers. The research is focused in the influence of the iron and copper losses on the winding resistances. An important measurement work on many transformer windings in the frequency domain made possible to draw conclusions about the behavior of the magnetic field and the representation of the losses in a circuit model. © 2000 Elsevier Science S.A. All rights reserved.

Keywords: Power transformers; Electromagnetic transient analysis; Resonance; Losses; Eddy currents; Winding impedances

1. Introduction

The results of an exhaustive experimental research about transformer winding impedances are shown in this paper. On this basis it was possible to draw conclusions not only about the losses but also about the inductances.

Winding resistances influence the damping during resonance. The characteristics of the resistance matrices were considered a very important question. One characteristic is the magnitude of the matrix, that can be characterized by the sum of all elements, and the other characteristic comes from the relations between the different elements of the matrix, that can be represented either by the magnitude of the short-circuit resistances of all coil pairs or by the differences between the different elements of the matrix.

Regarding the behavior of the winding, it will be shown that the magnitude of the resistance matrix has almost no significance. Otherwise, the relations between the different elements of the matrix are very important, since they determine the damping of the winding during transients.

Damping is strongly related to the leakage field. This can explain the similarity of the damping of windings with and without iron core, in spite of the fact that the order of magnitude of the resistance matrices is very different.

Research work related to impedance measurements at high frequencies has been done in the past [1]. The resulting conclusions, that should be valid for frequencies above 10 kHz, are:

1. The presence of the joke does not influence the inductances of the winding.
2. The interior of the iron core remains flux free.
3. Eddy currents appear on the iron core surface.

The first and third asseverations are true, but the second is in general not true. This will be demonstrated in the following. For an arbitrary distribution of magnetomotive force, the iron core is not flux free, still for high frequencies [2]. The magnetic field is not rejected completely, as the research done by the authors in this paper shows.

2. Linear winding model

If the transformer winding is represented as a linear model, the following linear equation system can be written

* Corresponding author.

PII: S0378-7796(99)00081-4

$$\mathbf{u} = \mathbf{Z}\mathbf{i} \quad (1)$$

where **u**, is the branch voltage vector; **i**, the branch current vector; and **Z,** the impedance matrix.

The impedance matrix is a symmetric complex matrix. The diagonal elements can be directly measured. The off-diagonal elements can be determined through an indirect measuring procedure. This procedure consists in the impedance measurement of the series connection of both involved coils. The series connection of the two coils to be measured is such that the magnetic flux created by each coil has the opposite direction (Fig. 1). The wanted impedance can be calculated by means of the following formula:

$$Z_{ij} = \frac{Z_{ii} + Z_{jj} - Z_{Gij}}{2} \quad (2)$$

with

$$Z_{G_{ij}} = Z_{ii} + Z_{jj} - 2Z_{ij} \quad (3)$$

Z_{Gij}: opposite flux series connection impedance (or short-circuit impedance) of coils i and j. The resonance is characterized by a particular current distribution in the winding. The currents are distributed so that the total mmf is normally very low [3]. This means that the magnetic flux is meanly leakage flux. For an adequate modeling of the transformer winding during resonance it is necessary to represent correctly the short-circuit inductances (opposite flux series connection inductances) and the corresponding resistances of matrix **Z** [3]. This can be best achieved with Eq. (2).

The short-circuit impedances (Eq. (3)) contain the most important information of the impedance matrix. If short-circuit impedances remain constant, the magnitude of the elements of **Z** have almost no significance.

This curious and important property of winding impedance matrices can be recognized by means of a sensibility analysis of matrix $\mathbf{Z}^{-1}$ regarding introduced variations of leakage flux (variations in the differences between inductances) or in the mean flux (variations introduced in all elements). In the first case big differences in the elements of $\mathbf{Z}^{-1}$ can be observed, while in the second case the differences are very small.

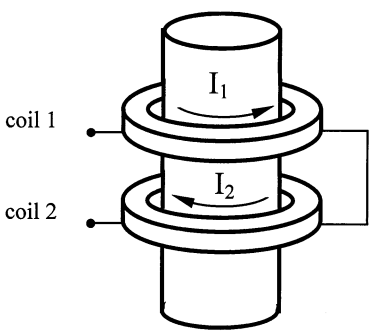

Fig. 1. Measurement of the impedance with an opposite flux series layout.

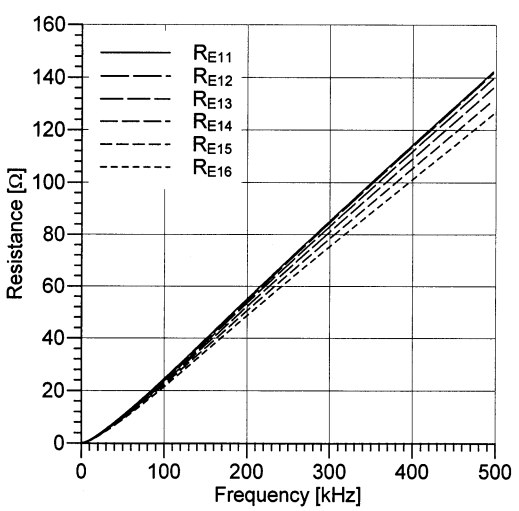

Fig. 2. Iron core winding resistances R_{E1k}: resistance of coils 1 and k, $k = 1,\ldots, 6$.

3. Winding impedances

Many measurements of the winding impedances variation with the frequency have been performed during the research work in a bandwidth of 1–500 kHz.

The measurements have been done by means of a HP 4192A impedance analyzer controlled by an IBM-compatible PC computer. The control software for the PC was the program HP_MESS [5].

An experimental winding was mounted over a PVC-tube, in which interior two different cores were used: a copper shield (not in short-circuit) and a laminated iron core. Ten normal disc coils made of rectangular cross-section and enamel-insulated copper wires were used to construct the winding. It has 20 turn per coil and a total of ten coils.

Impedance measurements have been performed for all impedances of both different layouts with a distance between coils of 1 cm.

The measurement results are shown in Figs. 2–5. Resistance and inductance curves in the figures correspond to coils 1 to k ($k = 1,\ldots, 6$).

The existence of an important main flux is evident from Figs. 2–4 (winding with iron core). The considerable influence of the iron losses becomes evident through the similarity of the curves shown in Fig. 2, that it is not the case for air core (Fig. 3)

In Fig. 4 can be seen that the magnetic flux in the core decreases almost linearly as the axial co-ordinate increases, since the distances between the curves of the inductances with iron core as a function of frequency are not so different. This behavior implies a large magnetic coupling between coils, and this is only possible when the main flux is strong.

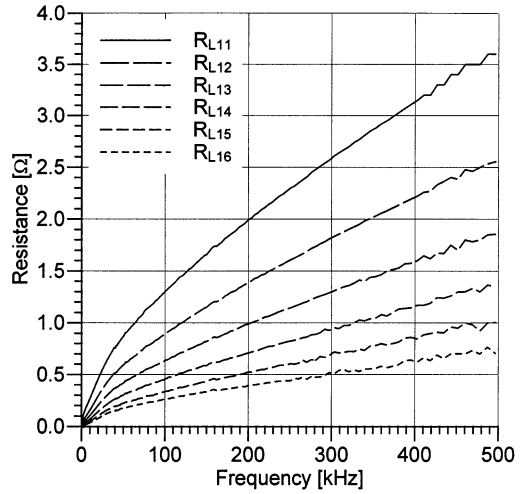

Fig. 3. Air core winding resistances R_{L1k}: resistance of coils 1 and k, $k = 1,\ldots, 6$.

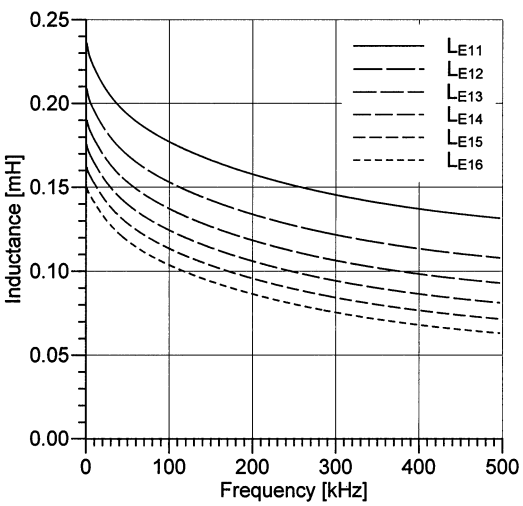

Fig. 4. Iron core winding inductances L_{E1k}: inductance of coils 1 and k, $k = 1,\ldots, 6$.

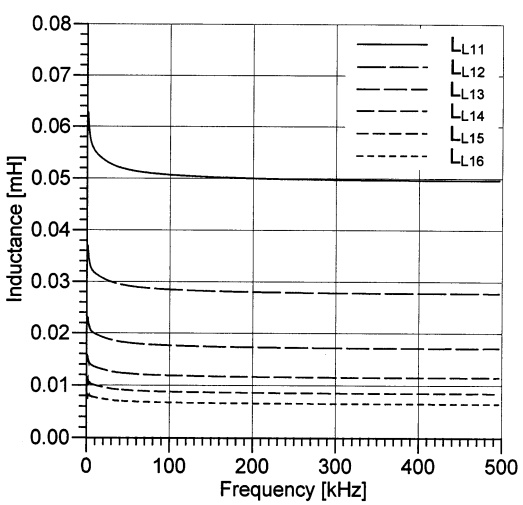

Fig. 5. Air core winding inductances L_{L1k}: Inductance of coils 1 and k, $k = 1,..., 6$.

The differences regarding the inductance curves for air core drawn in Fig. 5 are very important. The flux decreases here faster as the axial co-ordinate increases. The exponential decrease of the distances between curves makes it evident.

It can be mentioned that the curves of Fig. 2 and Fig. 4 have a considerably different form than the curves of Fig. 3 and Fig. 5. It is evident that in the case of windings with iron core more loss sources exist than in the case of windings with air core. This influences notably the variation of the impedances with frequency.

4. Impedances of different coil pairs for opposite flux series connection with and without iron core

The impedances of all coil pairs for the opposite flux series connection have been measured in order to have the data for the calculation of winding impedances by means of Eq. (2).

The frequency-dependent behavior of the real part of the impedances for the opposite flux series connection is shown in this paragraph in order to evidence the importance of the iron losses.

Figs. 6 and 7 show the behavior of these resistances with and without iron core. The different curves correspond to coils 1 and k, for $k = 2,\ldots, 6$.

The proximity effect in coils with circulating currents in opposite direction leads to a decrease in the resistance value of their series connection. This is true even for iron core layout, but this is only a secondary effect in this case. It is much more important here that for an opposite flux series connection only a small part of the flux penetrates the core, so that the iron losses are comparable with the copper losses.

It can be seen from the comparison of both figures that for small coil separations only small differences exist between resistances of both layouts. The greater the distance, the more different the resistances. Measured resistances of iron-cored coils rise by increasing coil separation. This behavior is due to the fact that the effect of the opposite flux series connection of both coils becomes unimportant, so that certain core flux is present again.

In spite of the fact that only a small part of the flux penetrates the core in the case of the opposite flux series connection, the iron and copper losses are of the same order of magnitude.

5. Winding voltages and resonance frequencies

Numerous measurements of winding voltages as a function of frequency have been performed for the cases of iron and air core using the experimental winding.

For the resonance frequencies of the experimental winding to be in the correct frequency range, the connection of capacitors between junction points of the coils and ground was necessary. It was considered as adequate a value of $C = 22$ pF for each capacitor (Fig. 8).

The winding nodes for which the maximal voltages appear and the corresponding voltage values are shown in Table 1. Measured overvoltages for iron and air core as well as the corresponding absolute and relative values are given. All voltages are related to the corresponding input voltage in p.u. values.

Table 2 shows the nodes for which the maximal voltages appear for each resonance frequency.

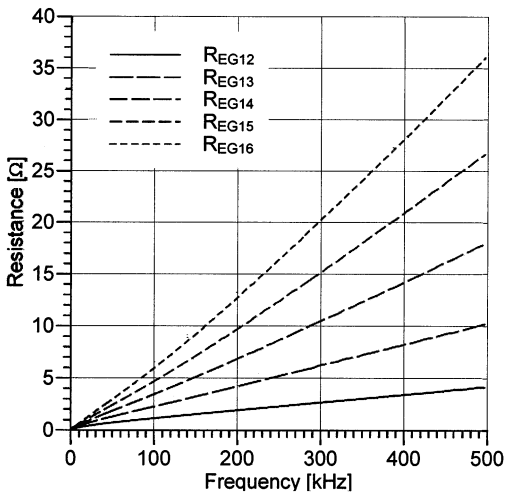

Fig. 6. Iron core resistances for opposite flux series connection R_{EG1k}: Resistance of coils 1 and k, $k = 2,\ldots,6$.

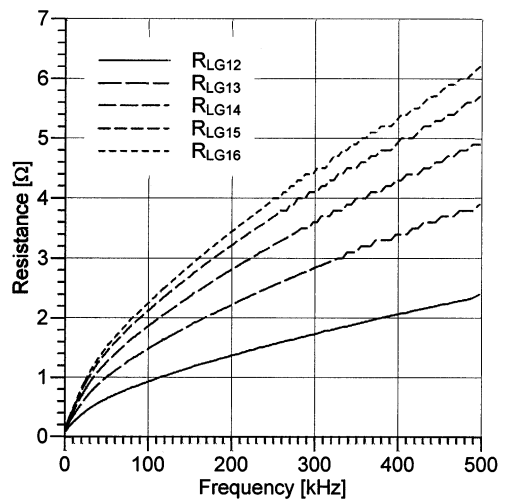

Fig. 7. Air core resistances for opposite flux series connection R_{LGlk}: Resistance of coils 1 and k, $k = 2,\ldots, 6$.

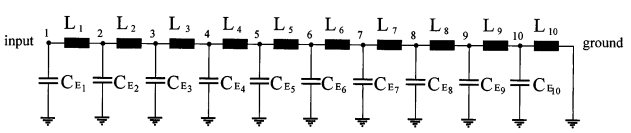

Fig. 8. Experimental winding equivalent circuit.

Figs. 9 and 10, respectively show the voltages of nodes four and six. From an analysis of these figures it becomes evident, that the *form* of the frequency response of both layouts are comparable despite the considerable differences of the parameters.

Table 1 shows the corresponding maximal voltage amplitudes and their relative differences. The resonance frequencies evidence certain deviations (see Table 2).

The smaller the resonance frequency order, the larger the difference between the maximal voltages of both cases (air and iron core).

Amplitude deviations appear for lower resonance frequencies, for which the highest overvoltages take place.

The differences of the respective short circuit inductances in both cases can be considered the cause of the observed deviations in the resonance frequencies.

With regard to the *maximal voltages* during resonance, the most important magnitudes are the resistances of the winding. The amplitude of the maximal voltages is not only dependent on the magnitude of the elements of the resistance matrix, but also on the relation between the different elements of this matrix. The damping of the winding increases for increasing resistances and for decreasing similarity of the elements of the resistance matrix. This can be explained as follows:

The resistive component of the voltage drop in the branch k can be represented as follows

$$u_{R_k} = \sum_{i=1}^{n} i_i R_{ki} \tag{4}$$

Eq. (4) can be written as

$$u_{R_k} = \sum_{i=1}^{n} i_i R_{ki} = R_0 \sum_{i=1}^{n} i_i + \sum_{i=1}^{n} i_i R'_{ki} \tag{5}$$

where $R_{ki} = R_0 + R'_{ki}$.

Under consideration of the approximate condition that branch currents cancel themselves during resonance, we have

$$\sum_{i=1}^{n} i_i \cong 0 \tag{6}$$

and the consequence is:

$$U_{R_k} \cong \sum_{i=1}^{n} i_i R'_{ki} \tag{7}$$

When the condition (6) is satisfied, the different terms of the first sum of the right side of Eq. (5) approximately neutralize. This means that Eq. (7) can be considered as a valid relation, no matter what the order of magnitude is of the elements of the resistance matrix.

Without this explanation it would be surprising, that the air-cored winding (lower resistances) has a similar damping as an iron-cored winding (very large resis-

Table 1
Maximal overvoltages

Eigenvalue	Nodes with the maximal voltage	Maximal voltage (p.u.) (air core)	Maximal voltage (p.u.) (iron core)	Relative difference (%)
1	6	8.58	8.81	−2.61
2	8	7.00	5.69	23.07
3	6	6.51	5.32	22.29
4	7	5.40	4.58	18.02
5	4	4.98	4.40	13.15
6	2	3.84	3.27	17.42
7	6	3.00	2.77	8.39
8	3	2.17	1.71	26.71
9	7	0.95	0.83	14.12

tances). This behavior has been investigated and explained by means of two numeric examples.

Since the magnetic flux during resonance is almost exclusively leakage flux, the exact representation of the core flux is not critical in this case.

6. Analysis of the influence of the resistance matrix

6.1. Winding models

The influence of the resistance matrix will be investigated by means of numerical examples. The purpose of the first example is to show that the absolute values of the resistance matrix elements have small influence during resonance. The second example shows how large the differences of resonance voltages can be, when two windings having different opposite flux series connection resistances are compared, even though the resistance matrix elements R_{ij} are not very unlike. The shown examples are based on a simplified model of the experimental winding using iron core [3].

The consideration of the frequency-dependence of resistances becomes necessary. The full occupied and frequency-dependent resistance matrix can be represented by means of the following simplified formulation:

$$\mathbf{R}(\omega) = \mathbf{R}_K \frac{a\omega^2}{1 + b\omega^2} \tag{8}$$

where $\mathbf{R}(\omega)$, frequency-dependent resistance matrix; $\mathbf{R}_K$, constant resistance matrix; a and b, parameters.

The form of the mathematical function of Eq. (8) is especially adequate for representing actual frequency-dependent resistances [3].

The election of the parameters included in Eq. (8) has been based in a frequency range of [0–150 kHz].

6.2. Example 1

The mathematical models of two different windings are analyzed in this example. The inductance and capacitance matrices L and C of the experimental winding without iron core characterize both models. For the sake of simplicity only constant inductances are used in all examples.

The first winding model (model 1) of this example is characterized by the following resistance matrix $\mathbf{R_1}$:

$$\mathbf{R_1} = \mathbf{R}_{K1} \frac{a\omega^2}{1 + b\omega^2} \tag{9}$$

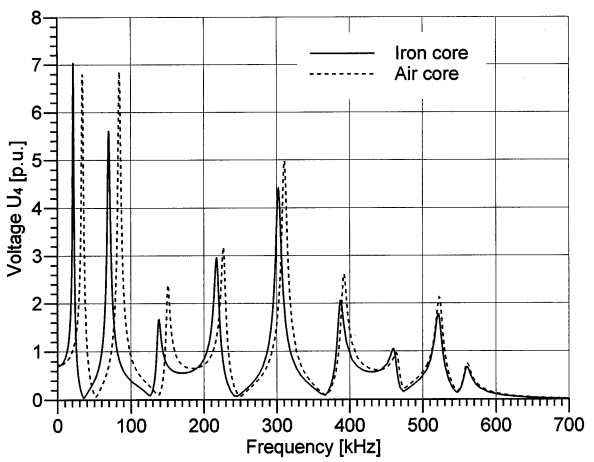

Fig. 9. Frequency response of node voltage U_4 related to the input voltage (amplitude).

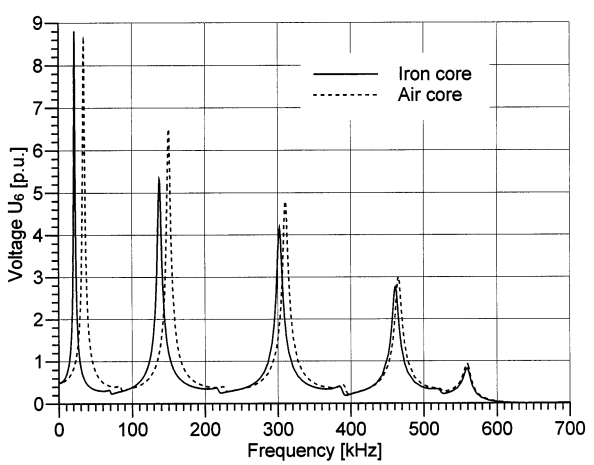

Fig. 10. Frequency response of node voltage U_6 related to the input voltage (amplitude).

Table 2
Nodes with maximal voltage at each resonance frequency

Eigenvalue	Nodes with the maximal voltage	Frequency (air core) (Hz)	Frequency (iron core) (Hz)	Relative difference (%)
1	6	34 237	21 555	58.83
2	8	84 355	69 935	20.61
3	6	150 150	137 530	9.18
4	7	226 910	217 680	4.24
5	4	310 370	302 370	2.64
6	2	391 630	386 540	1.32
7	6	465 150	461 290	0.84
8	3	523 120	522 190	0.18
9	7	558 390	559 050	−0.12

In this case the parameters are:

$$\mathbf{R_{K1}} = \begin{vmatrix} 1 & 0.993 & 0.9722 & 0.9444 & 0.9097 & 0.875 & 0.8333 & 0.7847 & 0.7291 & 0.6666 \\ 0.993 & 1 & 0.993 & 0.9722 & 0.9444 & 0.9097 & 0.875 & 0.8333 & 0.7847 & 0.7291 \\ 0.9722 & 0.993 & 1 & 0.993 & 0.9722 & 0.9444 & 0.9097 & 0.875 & 0.8333 & 0.7847 \\ 0.9444 & 0.9722 & 0.993 & 1 & 0.993 & 0.9722 & 0.9444 & 0.9097 & 0.875 & 0.8333 \\ 0.9097 & 0.9444 & 0.9722 & 0.993 & 1 & 0.993 & 0.9722 & 0.9444 & 0.9097 & 0.875 \\ 0.875 & 0.9097 & 0.9444 & 0.9722 & 0.993 & 1 & 0.993 & 0.9722 & 0.9444 & 0.9097 \\ 0.8333 & 0.875 & 0.9097 & 0.9444 & 0.9722 & 0.993 & 1 & 0.993 & 0.9722 & 0.9444 \\ 0.7847 & 0.8333 & 0.875 & 0.9097 & 0.9444 & 0.9722 & 0.993 & 1 & 0.993 & 0.9722 \\ 0.7291 & 0.7847 & 0.8333 & 0.875 & 0.9097 & 0.9444 & 0.9722 & 0.993 & 1 & 0.993 \\ 0.6666 & 0.7291 & 0.7847 & 0.8333 & 0.875 & 0.9097 & 0.9444 & 0.9722 & 0.993 & 1 \end{vmatrix}$$

where $a = 2.0\ \mathrm{e}^{-11}$; $b = 4.0\ \mathrm{e}^{-12}$.

It will be mentioned, that the matrix $\mathbf{R_1}$ is a simplified representation of the resistance matrix of the experimental winding with iron core.

Fig. 11 shows the frequency response of the resistance $R_1(1, 1)$ from Eq. (8).

The second winding model (model 2) is characterized by matrix $\mathbf{R_2}$, which is a modification of matrix $\mathbf{R_1}$:

$$\mathbf{R}_2 = \mathbf{R}_{K2}\frac{a\omega^2}{1+b\omega^2} \tag{10}$$

and

$$R_{K2_{ij}} = R_{K1_{ij}} + k \tag{11}$$

where $k = 999\ \Omega$.

$$\mathbf{R_{K2}} = \begin{vmatrix} 1000 & 999.9930 & 999.9722 & 999.9444 & 999.9097 & 999.8750 & 999.8333 & 999.7847 & 999.7291 & 999.6666 \\ 999.9930 & 1000 & 999.9930 & 999.9722 & 999.9444 & 999.9097 & 999.8750 & 999.8333 & 999.7847 & 999.7291 \\ 999.9722 & 999.9930 & 1000 & 999.9930 & 999.9722 & 999.9444 & 999.9097 & 999.8750 & 999.8333 & 999.7847 \\ 999.9444 & 999.9722 & 999.9930 & 1000 & 999.9930 & 999.9722 & 999.9444 & 999.9097 & 999.8750 & 999.8333 \\ 999.9097 & 999.9444 & 999.9722 & 999.9930 & 1000 & 999.9930 & 999.9722 & 999.9444 & 999.9097 & 999.8750 \\ 999.8750 & 999.9097 & 999.9444 & 999.9722 & 999.9930 & 1000 & 999.9930 & 999.9722 & 999.9444 & 999.9097 \\ 999.8333 & 999.8750 & 999.9097 & 999.9444 & 999.9722 & 999.9930 & 1000 & 999.9930 & 999.9722 & 999.9444 \\ 999.7847 & 999.8333 & 999.8750 & 999.9097 & 999.9444 & 999.9722 & 999.9930 & 1000 & 999.9930 & 999.9722 \\ 999.7291 & 999.7847 & 999.8333 & 999.8750 & 999.9097 & 999.9444 & 999.9722 & 999.9930 & 1000 & 999.9930 \\ 999.6666 & 999.7291 & 999.7847 & 999.8333 & 999.8750 & 999.9097 & 999.9444 & 999.9722 & 999.9930 & 1000 \end{vmatrix}$$

The relation between the respective matrix elements of both winding models is approximately 1:1000. The opposite flux series connection resistances of all coil pairs have the same values in both models:

$$R_{1G_{ij}} = R_{1_{ii}} + R_{1_{jj}} - 2R_{1_{ij}} \tag{12}$$

$$R_{2G_{ij}} = R_{2_{ii}} + R_{2_{jj}} - 2R_{2_{ij}}$$

$$= R_{1_{ii}} + k + R_{1_{jj}} + k - 2R_{1_{ij}} - 2k = R_{1G_{ij}} \tag{13}$$

The frequency response of node voltages of both models can be calculated from the given data.

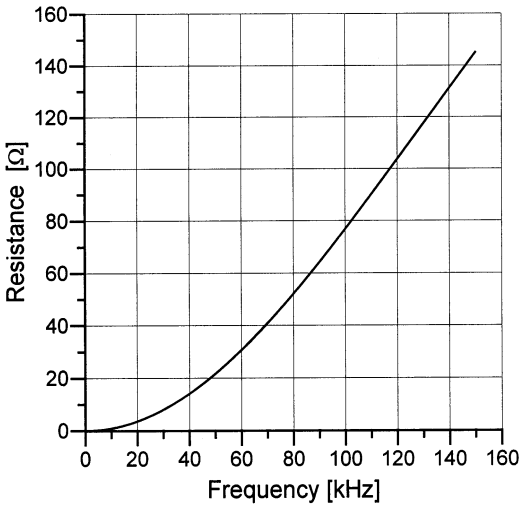

Fig. 11. Frequency response of resistance $\mathbf{R_1}(1, 1)$ (winding with iron core).

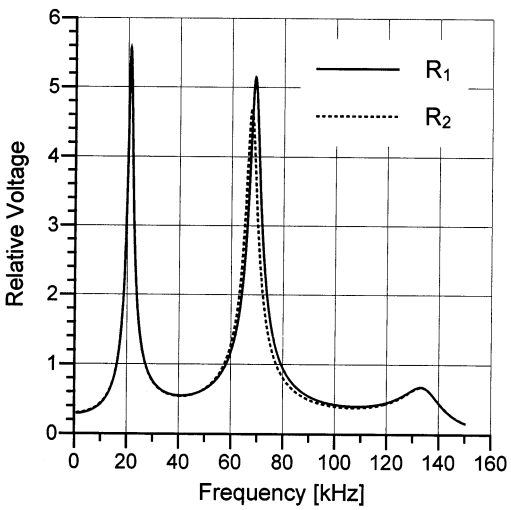

Fig. 12. Frequency response of voltage amplitude in node 8.

The behavior of both models was analyzed numerically in order to clearly evidence the influence factors regarding the damping. Fig. 12 shows the frequency response of the voltage in node 8. It becomes evident, that even though the order of magnitude of both resistance matrices is very different, the effective damping of both windings is very similar.

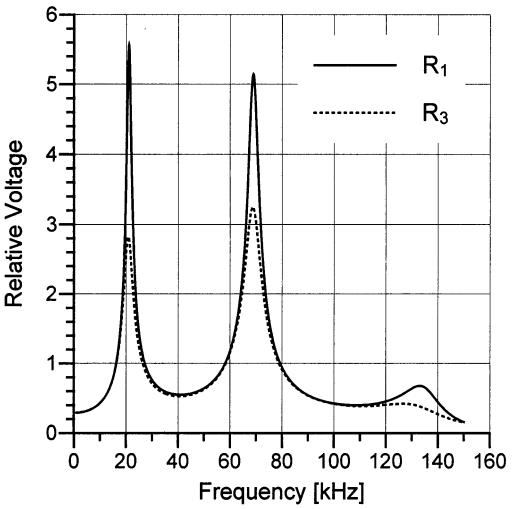

Fig. 13. Frequency response of voltage amplitude in node 8.

6.3. Example 2

In this example, model 1 ($\mathbf{R_1}$) is compared with a new winding model ($\mathbf{R_3}$). Winding model 3 has the same inductances as model 1. The resistances of model 3 are to be calculated as follows:

$$\mathbf{R_3} = \mathbf{R}_{K3}\frac{a\omega^2}{1+b\omega^2} \tag{14}$$

The value of R_{3Gij} is chosen to be the double of R_{1Gij}:

$$R_{3G_{ij}} = 2R_{1G_{ij}} \tag{15}$$

$$R_{3_{ii}} = R_{1_{ii}} \tag{16}$$

so that

$$R_{3_{ij}} = \frac{R_{3_{ii}} + R_{3_{jj}} - R_{3G_{ij}}}{2} \tag{17}$$

$$\mathbf{R_{K3}} = \begin{vmatrix} 1 & 0.986 & 0.9444 & 0.8888 & 0.8194 & 0.75 & 0.6666 & 0.5694 & 0.4582 & 0.3332 \\ 0.986 & 1 & 0.986 & 0.9444 & 0.8888 & 0.8194 & 0.75 & 0.6666 & 0.5694 & 0.4582 \\ 0.9444 & 0.986 & 1 & 0.986 & 0.9444 & 0.8888 & 0.8194 & 0.75 & 0.6666 & 0.5694 \\ 0.8888 & 0.9444 & 0.986 & 1 & 0.986 & 0.9444 & 0.8888 & 0.8194 & 0.75 & 0.6666 \\ 0.8194 & 0.8888 & 0.9444 & 0.986 & 1 & 0.986 & 0.9444 & 0.8888 & 0.8194 & 0.75 \\ 0.75 & 0.8194 & 0.8888 & 0.9444 & 0.986 & 1 & 0.986 & 0.9444 & 0.8888 & 0.8194 \\ 0.6666 & 0.75 & 0.8194 & 0.8888 & 0.9444 & 0.986 & 1 & 0.986 & 0.9444 & 0.8888 \\ 0.5694 & 0.6666 & 0.75 & 0.8194 & 0.8888 & 0.9444 & 0.986 & 1 & 0.986 & 0.9444 \\ 0.4582 & 0.5694 & 0.6666 & 0.75 & 0.8194 & 0.8888 & 0.9444 & 0.986 & 1 & 0.986 \\ 0.3332 & 0.4582 & 0.5694 & 0.6666 & 0.75 & 0.8194 & 0.8888 & 0.9444 & 0.986 & 1 \end{vmatrix}$$

For an actual winding, the relationships (15) to (17) should be valid even for the inductances. This means that winding model 3 should produce more leakage flux than model 1 (for example, by increasing coil separations).

Frequency response of voltage amplitude in node 8 is shown in Fig. 13. The damping behavior of both models is completely different, even though the elements of both resistance matrices $\mathbf{R_1}$ and $\mathbf{R_3}$ have similar orders of magnitude. By means of this example it becomes evident that the resistances R_G have considerable influence in the frequency behavior of the winding.

7. Conclusions

The comparison of the behavior of coils and windings with and without iron core leads to meaningful conclusions, which can be classified as follows:

- General conclusions
  1. The measured impedances of both layouts (iron core and air core) generally show large differences. The inductances of coils with iron core are much larger than the corresponding values of coils without iron core. The same conclusion is valid for the resistances.
  2. From this first point, it can be concluded that an important main flux can exist in the core even for high frequencies [2], *if the magnetomotive force distribution allows it*. The concept of 'complete shielding' or 'complete flux rejection outside the iron core' within the considered frequency range is wrong, since it contradicts the known fundamentals of the phenomena ([4], p. 338).
  3. Two types of differences exist between the impedances of both layouts. On one hand, the differences in order of magnitude of the impedances in both cases are more than evident from the measurements. On the other hand, more subtle differences exist between both cases regarding leakage flux. They become evident through the differences between the corresponding opposite flux connection impedances (or short-circuit impedances) of both winding layouts.
- Conclusions regarding resonance
  4. During the investigation it has been proved that the order of magnitude of the impedance amplitudes has a very small influence on the frequency response of winding voltages. Nevertheless, the differences between the distinct winding impedance matrix elements represent the most important factors of influence regarding the frequency-dependent voltage response of the winding.
  5. The mentioned relative differences between elements of matrix $\mathbf{Z}$ of a transformer winding with iron core have not the same values as in the case of a winding with air core. These relative differences have a close relation with the short-circuit impedances. The mentioned differences become evident by carefully observation of Figs. 2 and 3.
  6. The corresponding node voltage frequency responses of both cases can be considered as comparable, despite the differences in order of magnitude of the impedances. The differences in the short-circuit impedances comparing both cases cause, however, certain deviations in the low order resonance frequencies (different short-circuit inductances) and differences in the corresponding overvoltages (different opposite flux series connection resistances). The leakage flux distribution of a winding with iron core is not totally the same as in the case of air core. The consequence of this is that certain deviations arise.
  7. The mentioned conclusions can be summarized stating that leakage flux predominates during resonance. Under these conditions the magnetomotive force distribution is so, that the magnetic flux practically does not penetrate the iron core [3]. For this reason the iron losses are not an important factor during resonance.

The particular magnetomotive force distribution during resonance causes that the magnetic flux almost does not penetrate the iron core and it mainly becomes leakage flux.

References

[1] E. Buckow, Berechnung des Verhaltens von Leistungs-Transformatoren bei Resonanzanregung und Möglichkeiten des Abbaus innerer Spannungsüberhöhungen. PhD Thesis, Technische Hochschule, Darmstadt, Germany, 1986.

[2] J. Leohold, Untersuchung des Resonanzverhaltens von Transformator-wicklungen. PhD Thesis, Universität Hannover, Germany, 1984.

[3] E Mombello, Netzwerkmodell zur Darstellung des transienten Verhaltens des Transformators bei Resonanzanregungen mit Berücksichtigung der Verluste. PhD Thesis, Universidad Nacional de San Juan, Argentina, 1998.

[4] K. Küpfmüller, Einführung in die theoretische Elektrotechnik, thirteenth ed., Springer Verlag, Berlin, 1990.

[5] Martin Holle, Programmenentwicklung fur einen rechnergesteuerten Meßplatz zur Bestimmung von Frequenzgängen an Großtransformatoren. Bachelor Thesis, Institut für Allgemeine Elektrotechnik und Hochspannungstechnik, RWTH Aachen, Germany, 1989.